

Article

A Novel Through-Thickness Perfusion Bioreactor for the Generation of Scaffold-Free Tissue Engineered Cartilage

Eric Gilbert, Mark Mosher, Anuhya Gottipati and Steven Elder *

Agricultural & Biological Engineering, Mississippi State University, Starkville, MS 39762, USA;
E-Mails: eag67@msstate.edu (E.G.); mlm490@msstate.edu (M.M.); ag1208@msstate.edu (A.G.)

* Author to whom correspondence should be addressed; E-Mail: selder@abe.msstate.edu;
Tel.: +1-662-325-9107; Fax: +1-662-325-3853.

Received: 16 February 2014; in revised form: 2 May 2014 / Accepted: 30 July 2014 /

Published: 13 August 2014

Abstract: The objective of this study was to characterize our designed through-thickness perfusion bioreactor which could generate large scaffold-free tissue engineered cartilage constructs. The hypothesis being that through-thickness perfusion could accelerate maturation of scaffold-free tissue engineered cartilage, grown in transwell culture inserts large enough to repair typical size chondral lesions in the human knee. Internal cell culture media temperature and pH were examined over time, upon implementation of the bioreactor perfusion system inside a CO₂ incubator, to ensure adequate regulation conducive to cell viability. Results indicate that temperature and pH both equilibrate within approximately 3 h. The bioreactor was tested for its efficacy to support formation of 4.5 cm² constructs by porcine neonatal chondrocytes. Tests were conducted under three conditions: immediate perfusion with flow from bottom to top, immediate perfusion with media flow from top to bottom, and bottom to top perfusion after four weeks of static culture, giving the cells time to self-aggregate into a consolidated construct prior to perfusion. The best cell culture results were obtained when perfusion was delayed for four weeks relative to the immediate perfusion of the other methods, and this should be further investigated.

Keywords: perfusion; bioreactor; cartilage; scaffold-free

1. Introduction

Articular cartilage is an aneural, avascular connective tissue covering the end of diarthroidal joints that lacks the ability of self-repair. Once damaged, cartilage tissue degenerates and causes mobility problems for the individual as well as pain [1,2]. While the current medical methods used to repair the damaged or diseased tissue are adequate in maintaining a person's quality of life, they are insufficient in restoring the tissue to its native biochemical and biophysical properties [3,4].

Bioreactors in tissue engineering are used to help speed up the development of large constructs, as well as standardizing the results by regulating the environmental factors, such as pH, gas exchange, temperature, nutrient and growth factor transfer [5,6]. There are many types of bioreactors that are available for the creation of tissue engineered cartilage such as rotary wall vessel bioreactors like the RCMW™ produced by Synthecon Inc.®, or flow-around perfusion bioreactors like the C10-12 CartiGen™ bioreactor produced by Tissue Growth Technologies®, or hydrostatic pressure bioreactors like the CartiGen HP Bioreactor™ also produced by TGT®. Most bioreactors are designed to overcome the limitations of diffusional transport of nutrients and waste products, and some provide mechanical stimulus to promote ECM synthesis (e.g., hydrostatic pressure). Perfusion bioreactors have been shown to increase production of sulfated glycosaminoglycans, Type II collagen, as well as help the chondrocytes maintain their phenotype [7]. Potential advantages of a through-thickness perfusion bioreactor are better uniformity of flow through the developing tissue, with respect to depth and radius, as well as possibility of continuous monitoring of construct permeability via measurement of pressures within the bioreactor. With respect to this study, the hypothesis was that our through-thickness perfusion bioreactor could accelerate maturation of scaffold-free tissue engineered cartilage grown in transwell culture inserts large enough to repair the typical size chondral lesion in the human knee. While many studies generate tissue engineered cartilage constructs with the ultimate goal of repairing lesions of articular cartilage, the typical size of tissue engineered cartilage constructs is around 0.2 cm² (5 mm in diameter) [8–11]. However, arthroscopy studies reveal the average size of cartilage lesions to exceed 2 cm² [12,13]. Also the aforementioned bioreactors either produce cartilage constructs of inadequate size to repair a focal lesion in the human knee or they require a scaffold for cell growth [14]. The bioreactor described herein is designed to generate scaffold-free tissue engineered constructs with a circular area of 4.52 cm². The objective of this study is to characterize the bioreactor device in terms of equilibration response and uniformity of fluid velocity, in addition to pilot culture experiments to establish a proof-of-concept.

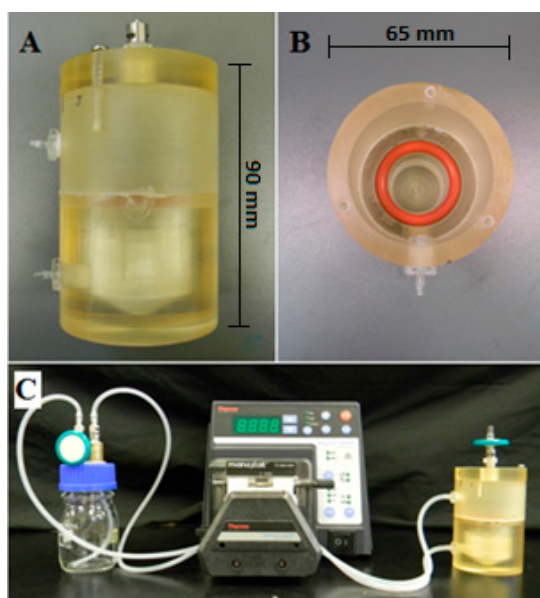
The benefit of using a scaffold-free tissue engineered cartilage construct is that the cell-to-cell interactions are similar to that of native articular cartilage and help to discourage the chondrocytes from dedifferentiating from their chondrogenic phenotype [15]. A previous study has shown that chondrocytes will self-aggregate into a cohesive construct through ECM deposition, thereby forming a neotissue which could potentially be used to repair a cartilage lesion [16]. The down side of the creation of a scaffold-free tissue engineered construct is the large number of chondrocytes required to generate a self-aggregating cartilage construct, although using a cell culture bioreactor could help to alleviate this problem. While there are currently many types of bioreactors employed to promote cell expansion such as spinner flasks and rotating wall vessel bioreactors, most rely on the use of a scaffold or hydrogel to organize the cells in three dimensions [17–20].

2. Experimental Section

2.1. Perfusion Bioreactor Design

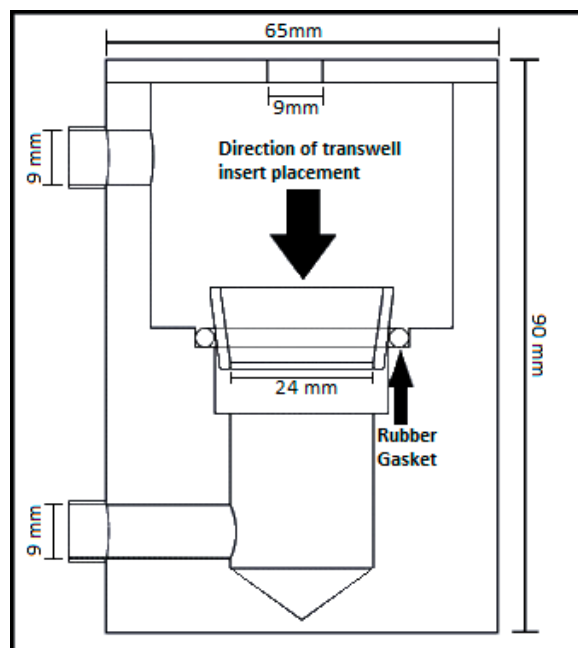
Our novel through-thickness perfusion bioreactor chamber (Figure 1) was designed as a cylindrical vertical flow chamber constructed of polysulfone. The center was hollowed out vertically so that, with a rubber gasket, a 6-well plate transwell insert would tightly fit into the chamber and ensure no flow of cell culture media around the insert (Figure 2). Most other perfusion bioreactors allow for the free unrestricted flow of media throughout the chamber [21]; this design restricts the flow to through the insert and thus through the cell construct. To transport media throughout the perfusion system, approx. 12 total feet of 2.78 mm diameter Manostat[®] silicon tubing was used to connect a 100 mL medium reservoir media bottle to inlet/outlet ports of the perfusion chamber. A Manostat[®] Carter[®] 4/8 Cassette Pump (Thermo Fischer Scientific, Waltham, MA, USA) was used to continuously pump 250 mL of cell culture media through the system. The bioreactor chamber was designed for media flow to ingress through the bottom port and egress out of the top port but by changing the peristaltic pump's direction of pumping the direction of flow can be reversed. Designing the system using a 150 mL polysulfone chamber and silicon tubing allows for the entire system sans pump to be steam autoclaved creating a sterile environment for cell culture. The experimental setup of the perfusion system allowed for all parts except for the peristaltic pump to be housed inside of a 37 °C, 5% CO₂ cell culture incubator. The Manostat[®] Carter[®] 4/8 Cassette Pump used was not manufactured for internal incubator use and as a result was set ontop of the incubator next to the external access port of the incubator. Silicon tubing was fed from the reservoir, across the pump, to the bioreactor chamber, and *vice versa* leaving approx. 8" of the 6' of tubing outside the incubator for both leads. Both the lid of the bioreactor chamber and lid of the media reservoir were fitted with 0.22 micron membrane filters to facilitate gas exchange with the 5% CO₂ atmosphere of the incubator.

Figure 1. Perfusion Bioreactor (A) Side view of the perfusion chamber; (B) Top down view of the perfusion chamber; (C) Representation of the bioreactor setup with peristaltic pump and media reservoir attached.



Before introducing cells, the length of time required for the bioreactor's temperature and pH to equilibrate was measured. This was done to both help further characterize the bioreactor and to ensure that there was no adverse side-effects to there being approx. 8" of tubing carrying media outside the incubator across the external pump from reservoir to bioreactor. The bioreactor chamber and reservoir were filled with 250 mL of Dulbecco Modified Eagle's Medium (DMEM), and the bioreactor was loaded into the incubator. Media was pumped through the system at 1 mL/min, and the temperature of media in the bioreactor chamber was continuously monitored using a thermocouple probe that fit tightly into the lid port meant for the 0.22 micron membrane filter. If any additional gas exchange was allowed by replacing the membrane filter with the thermocouple, it would not be expected to significantly affect temperature. Temperature readings were also taken from a 6-well plate containing 10 mL of DMEM with the thermocouple probe left in place with the lid removed. The small volume would be expected to equilibrate rapidly and it has a high surface area to volume ratio for gas exchange for temperature and pH comparison against the bioreactor. Temperature readings were taken every 15 min for the first hour and then every 30 min until equilibrium for both experiments. In a separate experiment, both vessels were in the incubator simultaneously using the same media volumes and flow speeds as in the respective temperature experiment for measurement of pH. pH measurements were taken repeatedly on the same volume within each vessel using an Orion 2-Star benchtop pH meter (Thermo Scientific, Waltham, MA, USA) every 15 min for the first hour and then every 30 min until equilibrium.

Figure 2. Cross-sectional diagram of the bioreactor chamber depicting the position of the transwell insert within the chamber.



2.2. Cell Isolation and Cell Culture

For each experimental method, neonatal porcine chondrocytes were freshly isolated from the stifle joints of four stillborn piglets donated by a local pig producer immediately after birth. For each experiment, the isolated cartilage from all piglets were collected together and digested in a 1 mg/mL Type II collagenase solution in DMEM containing 10% Fetal Bovine Serum (FBS) overnight at 37 °C

in an incubator with 5% CO₂. The cell suspension was passed through a 100 µm sieve and a cell count was conducted using a BioRad TC10™ Cell Counter with trypan blue to determine viability. A total cell suspension of 1.1×10^8 viable cells was evenly divided and immediately pipetted into two 6-well plate transwell inserts with a diameter of 24 mm giving each insert 5.5×10^7 viable chondrocytes.

In Method 1 the cell-laden transwell inserts were placed, one in the perfusion bioreactor chamber and one in an identical chamber for static culture, immediately after Type II collagenase digestion. The chondrocytes were cultured in Defined Chondrogenic Medium (DCM) made with DMEM containing 1% v/v ITS + Premix (BD Biosciences, San Jose, CA, USA), 0.1 µM dexamethasone, 1 mM sodium pyruvate, 50 µg/mL ascorbate-2 phosphate, 40 µg/mL L-proline, 1% v/v antibiotic-antimycotic solution (Sigma, St. Louis, MO, USA) and 10 ng/mL recombinant human TGF-β3 for ten days with one bioreactor chamber having continuous through-thickness perfusion of 1 mL/min with media changes at 5 days. The other transwell insert was in an identical bioreactor chamber but not connected to the pump and allowed to culture under static conditions for ten days with media changes at 5 days. The flow speed of 1 mL/min was selected because it was the lowest pump speed possible for the 2.79 mm tubing used to connect the bioreactor to the reservoir. The direction of media flow throughout the chamber was with flow ingress through the bottom port of the chamber and flow egress through the top port back to the reservoir as was intended and is common among bioreactors. At the end of the time period the constructs were tested mechanically and then sectioned for biochemistry and histology.

Method 2 was conducted after Method 1 in the same manner with immediate introduction of one 5.5×10^7 cell-laden transwell insert into the bioreactor and constant perfusion with DCM for ten days, but the direction of perfusion was reversed allowing for ingress of flow through the top port and egress of flow through the bottom port of the bioreactor chamber (opposite of the first experiment) at 1 mL/min. Another transwell insert also containing 5.5×10^7 viable neonatal porcine chondrocytes was placed in an identical bioreactor chamber with DCM but without perfusion to serve as a static culture control. After ten days of cell culture with media changes at 5 days both constructs were tested mechanically and then sectioned for biochemistry and histology.

In Method 3, conducted after Method 2, a suspension of 5.5×10^7 viable cells was pipetted into each of two 6-plate transwell inserts and both were cultured under static conditions for 28 days in 100 mL of DCM with media changes every four days. After this time period one insert was randomly chosen and placed in the perfusion bioreactor and cultured under continuous 1 mL/min bottom-to-top directional perfusion (same directional flow as Method 1) while the other was placed in an identical bioreactor chamber and maintained under static conditions for ten days. At the end of the ten day time period the constructs were tested mechanically and then sectioned for biochemistry and histology.

2.3. Biomechanics and Biochemistry

At the end of each cell culture experiment, each construct, perfused and static, was immediately tested biomechanically at six non-overlapping locations around the construct for Young's elastic modulus using unconfined compression by indentation testing using a Mach-1 Micromechanical Testing System (Biomomentum, Laval, QC, Canada). The thickness was first determined by finding contact with the construct under a force of 5 grams. Then a ramp load was applied to 25% compressive strain

at a rate of 5 $\mu\text{m/s}$ and the force was monitored until the relaxation rate dropped below 0.1 g/min . The Young's modulus was calculated using the following equation:

$$E = \frac{F(1 - \nu)}{2ka\omega_0} \quad (1)$$

where F is the applied load or in this case the equilibrium force, $\nu = 0.3$ is Poisson's ratio, k is a scaling factor (a function of the aspect ratio (a/h) and ν), ω_0 is the indenter displacement, $a = 2.14$ mm is the radius of the indenter, and h is the thickness of the sample [22]. The scaling factor, k , was obtained from a previous study done by Haynes *et al.* [23].

After biomechanical testing twelve samples from each construct were collected using a 4 mm biopsy punch, six for hydroxyproline content and six for glycosaminoglycan (GAG) content. Total hydroxyproline content was measured as an indicator of collagen content and determined by the Chloramine T assay established by Reddy and Enwemeka [24]. Each sample's hydroxyproline content was normalized to the DNA content of the corresponding sample. For GAG content, each sample was digested overnight at 60 °C in a 50 mM sodium acetate (pH 6) solution containing 1% papain. Dimethylmethylene blue (DMB) solution was prepared according to Hoemann [25]. After adding 250 μL of DMB to 15 μL of papain digestate, the absorbance was read at 530 nm and 590 nm using a BioTek μQuant Microplate Spectrophotometer (BioTek Instruments, Winooski, VT, USA). A standard curve was constructed using chondroitin sulfate by plotting ($\text{OD}_{530} - \text{OD}_{590}$) against the known GAG concentration. DNA content in the same papain-digested sample determined using the DNA Quantitation Kit, Fluorescence Assay (Sigma, St. Louis, MO, USA) according the manufacturer's instructions. GAG content was normalized to DNA content and reported as $\mu\text{g}/\mu\text{g}$.

Statistical analysis of the biomechanical and biochemistry data was performed between the static and perfused groups for each method. Analysis was done using Microsoft Excel 2013™ with a two-tailed t -test assuming unequal variance ($\alpha = 0.05$).

2.4. Histology

For Methods 1 and 2, samples were fixed in neutral buffered formalin and embedded in paraffin. To display proteoglycan concentration sections (5 μm) were stained with 2% wt/vol Toluidine blue in 1% v/v acetic acid and counterstained with Wiegert's hematoxylin. Additional sections were immunostained for detection of Type II collagen according to previously published methods [8]. Images were captured using a Leica DM 2500 microscope (Leica Microsystems Incorporated, Bannockburn, IL, USA). Histology of Method 3 is unavailable due to mishandling during processing.

2.5. Modelling

A simplistic computational fluid flow model was created using the FloExpress plugin of SolidWorks to help further characterize the bioreactor and observe what types of pressures were occurring inside the bioreactor across the membrane of the transwell insert for the flow velocity used in the experiments. The first model was designed to be the bioreactor chamber with the transwell insert being empty as a control to get a base value of the pressures exhibited inside the bioreactor during the experiments. Boundary conditions of the inlet and outlet were set to 1 mL/min using water as a cell culture media

analog with a direction of flow from bottom to the top. The model was simulated assuming laminar flow, accounting for gravity, for 400 iterations leading to a convergent solution.

The second model used all assumptions and boundary conditions from the first model but accounted for the membrane of the transwell cell culture insert containing neonatal cartilage cell suspension as would occur early in the experiment. The cell suspension was modelled as a 1 mm thick layer in the bottom of the transwell insert to which physical properties were assigned in the engineering database of SolidWorks. The layer, which represented the mass of chondrocytes shortly after aggregation, was assigned a permeability coefficient characteristic of multipotent mesenchymal tissue as determined by Loba *et al.* [26]. The pressure differential across the cell suspension was estimated using the equation following Darcy's Law (2).

$$v = k \left(\frac{\Delta P}{\mu \times \Delta x} \right) \quad (2)$$

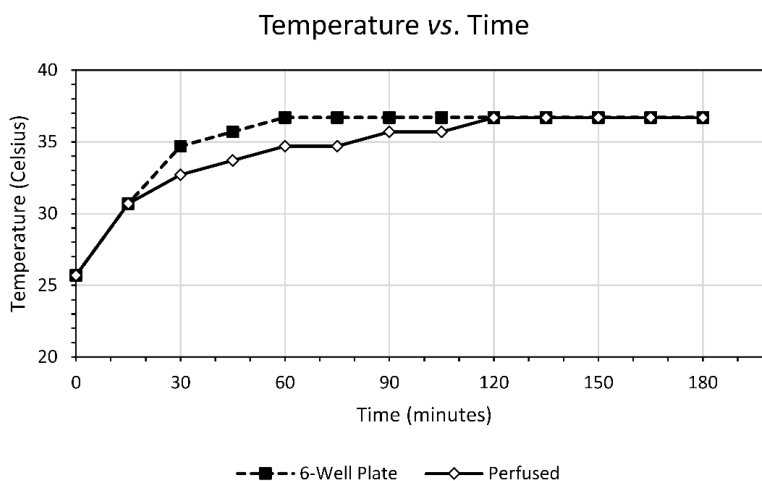
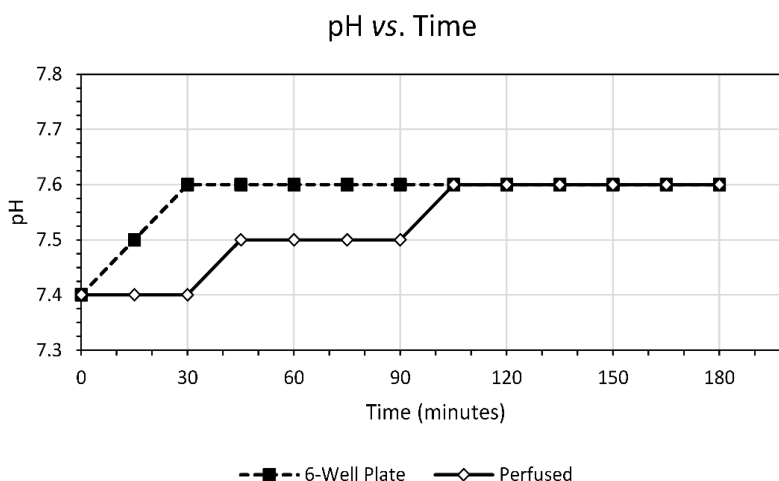
Here, v is the volumetric flowrate set at 1 mL/min, k is the permeability constant obtained from Loba *et al.* to be $1 \times 10^{-13} \text{ m}^4/\text{N}\cdot\text{s}$ for multipotent mesenchymal tissue, μ is the dynamic viscosity of water at 37 °C which is 686.5 Pas, and Δx is the thickness of the cell suspension which is 1 mm. The model was run and calculations repeated for 400 iterations leading to a convergent solution.

The third model was created using all assumptions and boundary conditions from the first model but adding a boundary condition at the transwell membrane to account for an engineered construct with properties approaching those of native cartilage. A 1 mm thick layer was created at the membrane of the transwell insert to represent a cartilage construct, and physical properties were assigned in the engineering database using the same equation from model two. In this model the permeability coefficient was $4.8 \times 10^{-15} \text{ m}^4/\text{N}\cdot\text{s}$, which is the permeability coefficient of articular cartilage [26]. This was used in conjunction with Darcy's Law as in model two.

3. Results and Discussion

3.1. Bioreactor Design

As can be seen in Figure 3, the temperature test shows that the 6-well plate equilibrates to the internal incubator temperature more quickly than the perfusion bioreactor chamber as would be expected. The perfusion chamber takes at least two hours for the temperature to equilibrate to the incubator and as such should be allowed to sit in the incubator for this time frame before introduction of cell culture. Figure 4 shows that pH tended to stay within a narrow range close to the accepted cell culture pH value of 7.4 which is supported by the fact that for both the 6-well plate and the perfusion chamber there was no perceptible change in the color of the DMEM. Also as expected, the 6-well plate reached the equilibrium pH of 7.6 at 30 min whereas it took over 100 min for the perfusion bioreactor chamber to reach the same value. This indicates that there is adequate gas exchange in both the perfusion bioreactor and media reservoir.

Figure 3. Line graph showing Temperature over Time.**Figure 4.** Line graph showing pH over Time.

3.2. Cell Culture

On gross appearance, the Method 1 perfused construct was substantially thicker and less opaque than its statically cultured counterpart shown in (C) of Figure 5. This appearance was in contrast to those of the Method 2 and Method 3 perfused constructs which were both more homogeneously opaque than the statically cultured constructs. It should be noted that most of the neotissue formed in the non-perfused control to Method 2 contracted into a dense lump. The Method 3 perfused construct was by far the most firm and easily handled tissue, and its surface was noticeably smoother.

As seen in Table 1 the Young's modulus of the Method 1 perfused construct was significantly lower than the non-perfused control. Interestingly, the amount of GAG and DNA accumulated on a per cell basis was not different from that of the non-perfused control, indicating the ECM of the perfused construct was much less dense. The spatially-averaged biochemical properties of the non-perfused and Method 2 perfused constructs were not significantly different. Yet due to the small contracted shape of the static construct, the sample had to be cut with a straight razor to provide a smooth surface of the indenter to fully engage for thickness and stress relaxation tests. As a result no true thickness for the static construct could be reported and the value for the Young's modulus was averages over only two

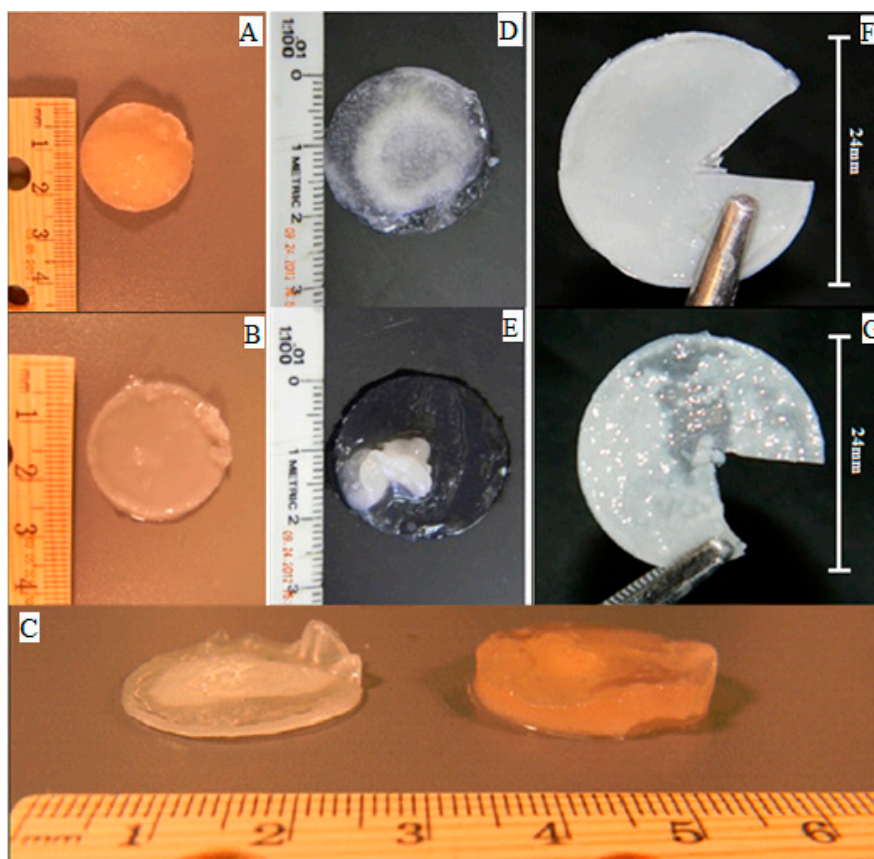
different locations. Despite the small size of the construct, the sample size for the biochemistry was not affected. The Method 3 perfused construct displayed a significantly higher Young's modulus than the non-perfused control. Normalized to DNA, the spatially-averaged collagen and GAG contents were higher and lower, respectively, than the non-perfused counterpart. However, the sample sizes were too small to demonstrate that these differences were statistically significant.

Table 1. Biochemical and biomechanical data of cartilage constructs from all experiments.

Experiment	Media Flow	Construct Thickness (mm)	Young's Modulus (kPa)	Hydroxyproline/DNA ($\mu\text{g}/\mu\text{g}$)	GAG/DNA ($\mu\text{g}/\mu\text{g}$)
Method 1	Static	0.79 (± 0.056)	46.6 (± 2.4)	0.0347 (± 0.0033)	0.1199 (± 0.0272)
	Perfused	3.05 (± 0.36) *	2.4 (± 1.0) *	0.0332 (± 0.0010)	0.1441 (± 0.0836)
Method 2	Static	n/a	21.0 (± 5.7) **	0.0353 (± 0.0022)	0.0398 (± 0.0078)
	Perfused	0.944 (± 0.287)	15.8 (± 12.1)	0.0328 (± 0.0045)	0.04452 (± 0.00454)
Method 3	Static	0.43 (± 0.302)	37.6 (± 12.7)	0.301 (± 0.040)	100.10 (± 24.6)
	Perfused	0.524 (± 0.0622)	86.6 (± 23.9) *	0.354 (± 0.080)	75.17 (± 5.0)

* Indicates statistically significant difference with respect to static culture; ** Indicates small sample size.

Figure 5. (A) Gross morphology of Method 1 perfused cartilage construct; (B) Gross morphology of Method 1 static cartilage construct; (C) Gross comparison of the differences in thickness between static and perfused constructs of Method 1; (D) Gross morphology of Method 2 perfused cartilage construct; (E) Gross morphology of Method 2 static cartilage construct; (F) Gross morphology of Method 3 perfused cartilage construct; (G) Gross morphology of Method 3 static cartilage construct.



The additional sections for Methods 1 and 2 were toluidine blue stained to determine proteoglycan content and separately stained for Type II collagen. The static histological sample for Method 2 showed a positive staining in both Type II collagen (Figure 6) and Toluidine blue (Figure 7). This indicates that in the static construct of Experiment Two there is the presence of proteoglycan content and of Type II collagen throughout the construct. The perfused construct in Method 2 stained moderately for Type II collagen and Toluidine blue. The staining on the perfused construct of Method 2 indicates the presence of Type II collagen and contains an ECM with positive proteoglycan content. For Method 1, both the static and perfused constructs stained with similarly moderate intensities for both Type II collagen and Toluidine blue. This indicates that there is not much difference in the positive amount of proteoglycan content between the two constructs as well as with Type II collagen. The air capsule displayed in both the Toluidine Blue and Type II collagen staining of perfused histology of Method 1 is not an artifact from processing but a result of the high shear stresses on the cells due to immediate perfusion [27].

Figure 6. Type II collagen histology from Methods 1 and 2. (A) Method 1, Static; (B) Method 1, Perfused; (C) Method 2, Static; (D) Method 2, Perfused. * all scale bars are 500 μm .

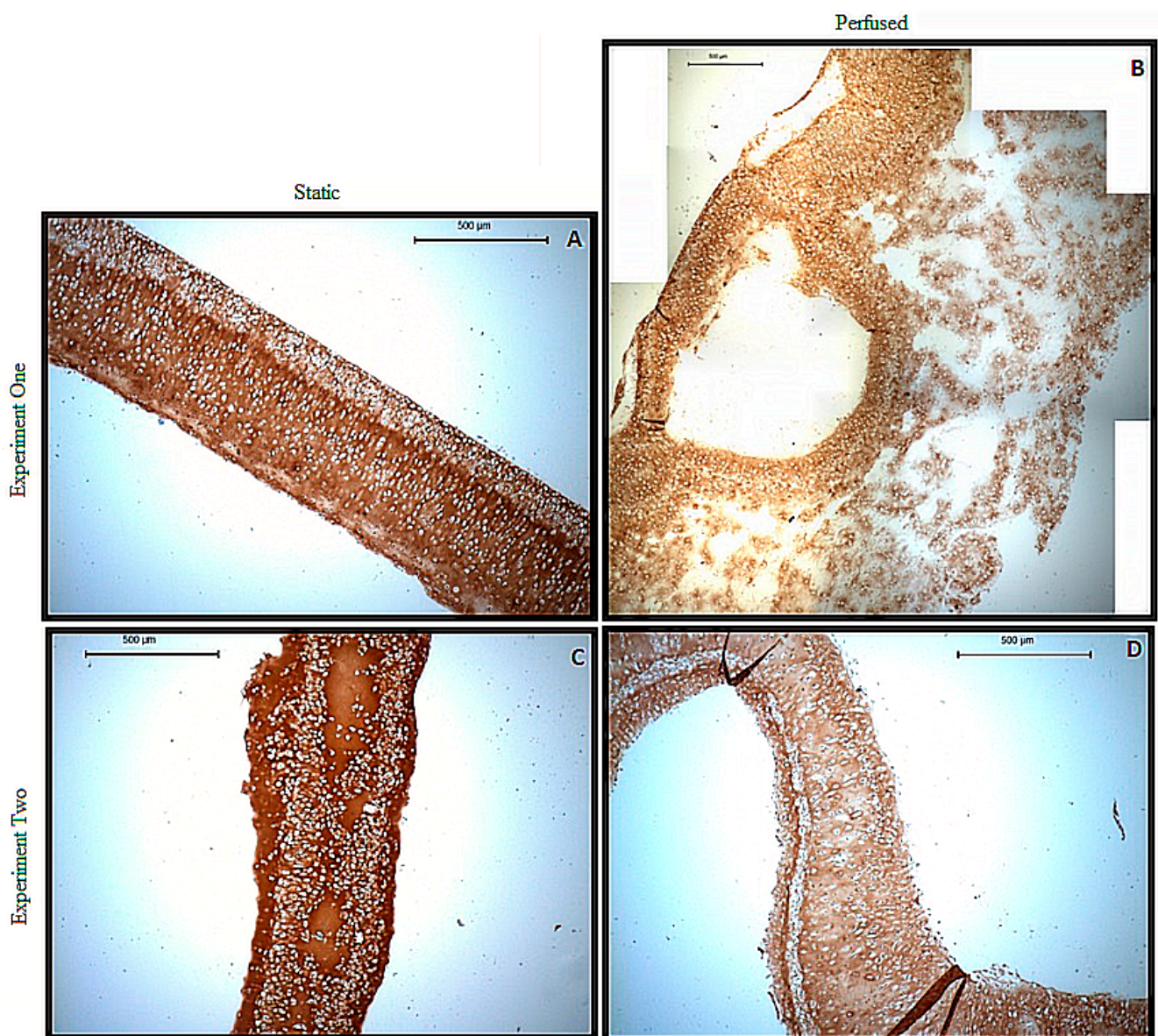
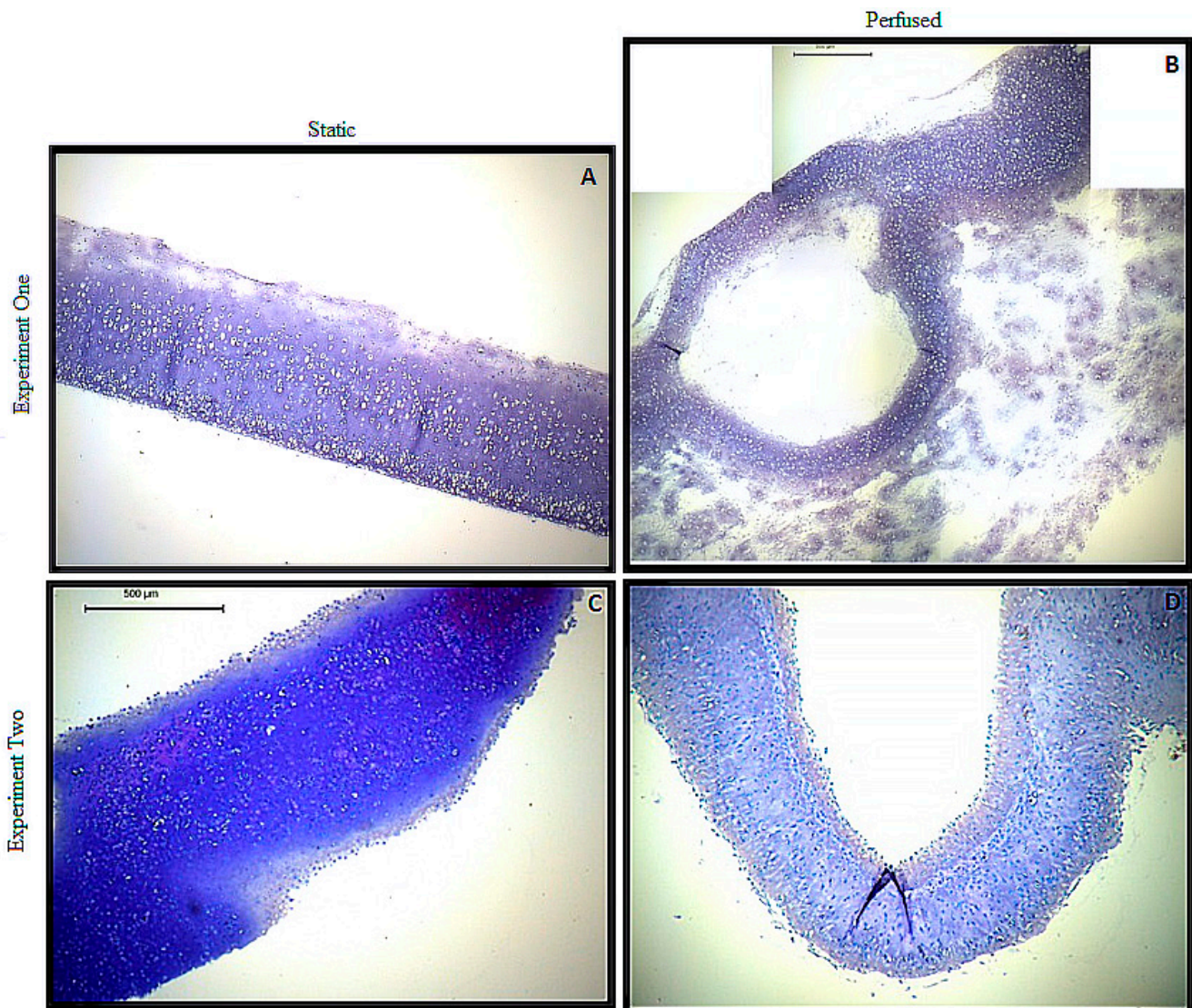


Figure 7. Toluidine Blue histology from Methods 1 and 2. (A) Method 1, Static; (B) Method 1, Perfused; (C) Method 2, Static; (D) Method 2, Perfused. * all scale bars are 500 μm .



3.3. Modelling

The second computational fluid model (Figure 8C) with the cell suspension analog, as would be expected early in the experiment, displayed pressures similar to that of the model of the empty bioreactor. Both models showed an absolute pressure across the membrane of approximately 102.70 kPa below the transwell insert and an absolute pressure ~ 98.0 kPa above the transwell insert. The absolute pressure values from above and below the transwell insert of the second model indicate that there is an upward 2.13 N acting against the membrane of the insert yet is not enough to dislodge the insert from the rubber gasket ensuring through-thickness perfusion. The third computational fluid model with the articular cartilage analog (Figure 8D), used to describe the end of the experiment, displayed absolute pressures of ~ 123.90 kPa below the transwell insert and ~ 98.0 kPa above the transwell insert. The differential pressure values from above and below the transwell insert of the third model indicate that there is an upward 11.67 N acting on the insert and could be enough to dislodge the insert but not until the permeability of the perfused construct is similar to that of native articular cartilage.

Figure 8. (A) Schematic of the bioreactor chamber with transwell in SolidWorks® (units in mm); (B) Surface contour plot of empty bioreactor; (C) Surface contour plot of bioreactor with simulated cell suspension in transwell insert; (D) Surface contour plot of bioreactor with simulated articular cartilage in transwell insert.

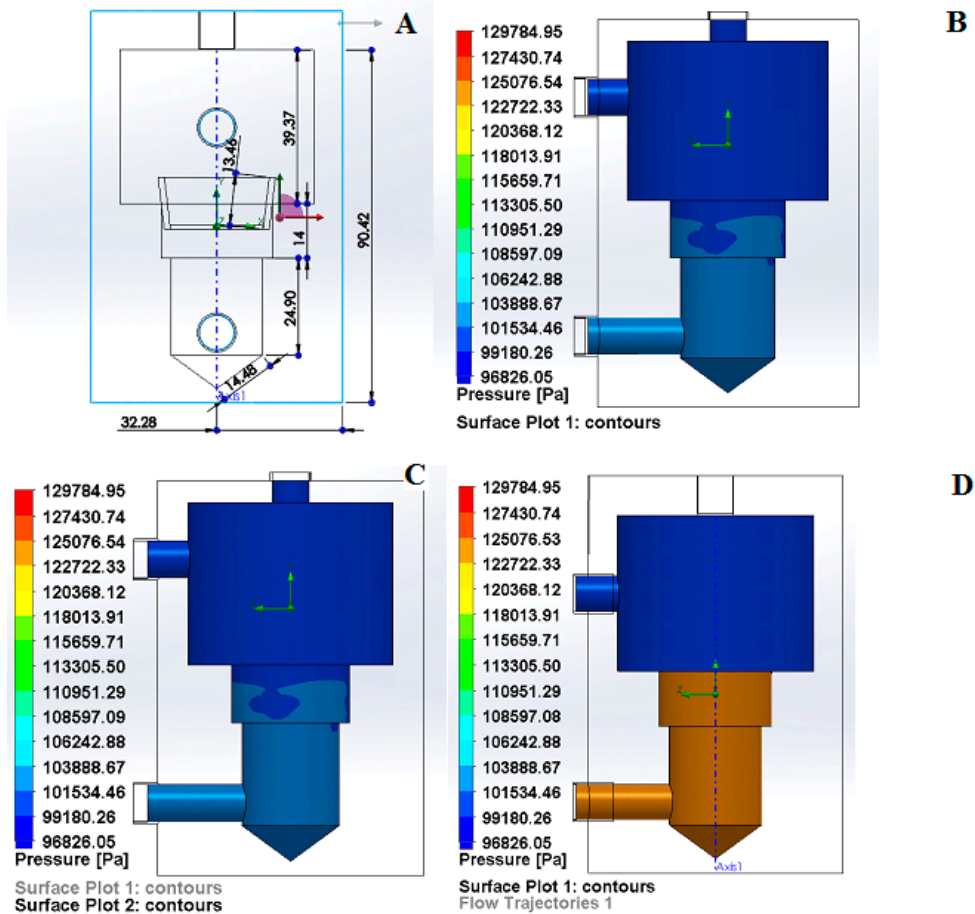
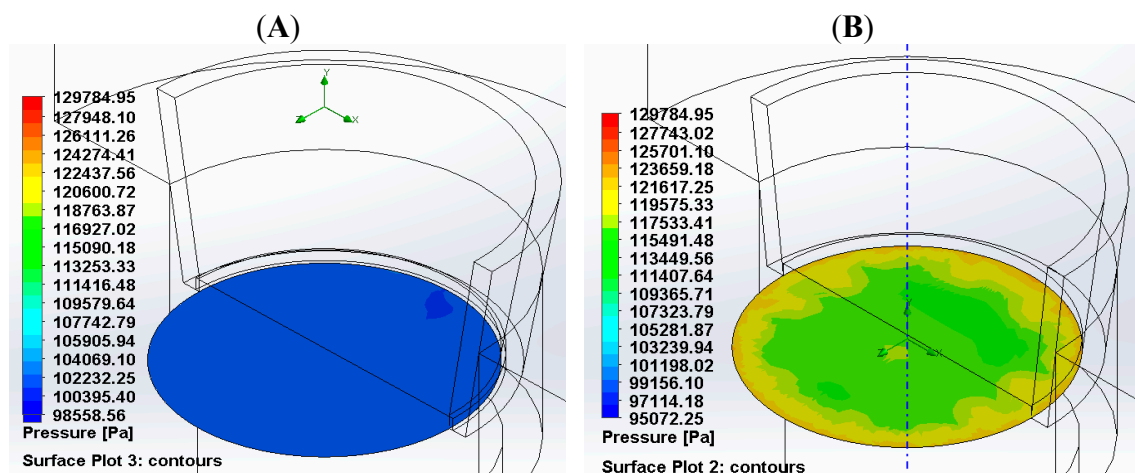


Figure 9. (A) A surface plot depicting the absolute pressure occurring radially across the transwell insert membrane having cell suspension permeability; (B) A surface plot depicting the absolute pressure occurring radially across the transwell insert membrane having articular cartilage permeability.



According to Figure 9, there is an inverse relationship between the permeability of the cartilage construct and the change in pressure across the width of the transwell insert membrane assuming a flow rate of 1 mL/min. As the permeability of the cartilage construct decreases due to the deposition of extracellular matrix under perfusion the variability of pressure across the transwell insert membrane increases. Also the pressure increases across the membrane are drastic between the bioreactor with cell suspension and bioreactor with articular cartilage with each having ΔP of 1682.81 Pa and 3893.64 Pa respectively.

3.4. Discussion

The design of the bioreactor is successful in achieving through-thickness perfusion by means of a rubber gasket which captures a 2.4 cm diameter transwell insert such that cell culture media cannot flow around it. The only channel through which pump driven culture media can flow is through the insert's membrane in a direction perpendicular to the thickness of a layer of cells settled on top of the membrane. The bioreactor is also successful in temperature and pH regulation as indicated by the results. These two factors were examined for two reasons with the first being that the pump being external to the cell culture incubator causes some stretch of tubing carrying media to also be outside the incubator and thus exposed to ambient temperature. The temperature results show that the internal temperature of the bioreactor chamber is a nonissue due to the pumps slow rate of speed coupled with the large volume of media. The second factor causing observation of the pH of the bioreactor chamber was because upon implementation of the transwell insert into the bioreactor, the entire system is sealed with the only access to the environment being through the 0.22 micron membrane filters fitted to the bioreactor lid and media reservoir lid. As the pH results indicate there is ample gas exchange throughout the system. The design of the bioreactor also allows for changing media by simply exchanging cell media reservoirs, which minimizes the chance of microbial contamination. When media was changed at the previously specified time points (5 days) there was no perceptible color change in the media indicating that the presence of the chondrocytes had no adverse effects on the pH of the system other than would be expected in a normal cell culture system. The major limitation of the current bioreactor prototype is the minimum flow rate achievable using 2.79 mm tubing. Slower flow rates can be easily attained by using smaller diameter silicon tubing while maintaining the same pump speed. For example, the use of 0.19 mm diameter tubing at a pump speed of 10 rpm should yield a flow rate of approximately 13.0 $\mu\text{L}/\text{min}$. This should be further investigated since other perfusion studies use a wider range of perfusion velocities [28,29].

Each method was done sequentially and the results were examined after each method. This had a heavy impact on how the experimental methods of each experiment were conducted. Method 1 was conducted in the standard practice using bottom to top directional immediate perfusion to determine what effect was had on scaffold-free tissue engineered cartilage. But upon examination of perfused histology of Method 1, the immediate perfusion caused too much shear stress for the chondrocytes to be able to handle (even at the lowest pump setting). As a result the direction of flow was reversed for Method 2 so that the cell suspension would be under compression due to the top to bottom directional flow of media against the transwell insert membrane. While the results of Method 2 did produce a perfused cartilage construct with superior biomechanical properties than that of Method 1, the construct

as a whole was not as homogeneous as would be needed to repair a focal lesion in the human knee (Figure 5D). This led to Method 3 having the perfusion of the cells delayed and the cells allowed to grow in static culture so that they could aggregate into a self-cohesive construct that could withstand the shear forces of bottom to top directional perfusion. This direction of perfusion was decided upon for Method 3 because the top to bottom perfusion of Method 2 posed the risk of media overflow from the chamber where the direction of flow in Method 1 was aided by gravity siphoning and overflow was not an issue. We speculated that the perfusion rate of 1 mL/min might still be advantageous if its onset was delayed until the construct had matured and had acquired a denser ECM with lower permeability.

This study also demonstrates that the bioreactor can accelerate development of scaffold-free engineered cartilage. Perfusion of porcine chondrocytes which had self-assembled during a 28-day period of static culture significantly increased the equilibrium Young's modulus in compression (Method 3). While the final modulus is still far from that of articular cartilage, it is assumed that the modulus would have continued to increase with increasing perfusion duration. Qualitatively, perfusion produced a very homogeneous construct with uniform thickness and smooth surface. The ability of chondrocytes to self-assemble into three-dimensional cartilage in the absence of a scaffold has been demonstrated previously [15], and this study suggests that maturation of such constructs can be enhanced by through-thickness perfusion. Our results also suggest that immediate perfusion of a chondrocyte layer can interfere with chondrogenesis if the flow rate is too high causing void pockets or capsules throughout the tissue [26]. This was the case with the perfused construct of Method 1 upon examination of sections under a microscope and explains both the thickness and the low elastic modulus of the construct. Reversing the direction of flow mitigated the detrimental effects, but it did not lead to an enhancement of properties at a flow rate of 1 mL/min. While the histology of the static construct from Method 2 is more intensely stained for Toluidine blue than its perfused counterpart, this is not a clear indicator of more proteoglycan content. The metachromatic staining of the perfused and static constructs of Method 2 is similar, indicating similar proteoglycan content which is supported by biochemical data.

Currently most cartilage bioreactors focus on applying different types of mechanical loads such as hydrostatic pressure, compression, shear, or some combination thereof [30,31]. Our bioreactor can apply depending on the direction of perfusion either shear or compression and shear evenly across the width of the construct according to the results of the computational fluid model. Also our bioreactor can apply these forces directly to the construct using through-thickness perfusion as opposed to passive application of by-flow media used in most other bioreactors [17,18]. By using through-thickness perfusion on a statically conditioned construct the thinnest areas become the path of least resistance encouraging more flow with higher shear stresses. As shown in previous studies this encourages more ECM production, especially collagen, in those regions and could overall produce a more homogeneous construct with the capacity to develop into a construct capable of repairing a lesion [32–34].

Moving forward with these results, it is apparent that a period of static culture is needed to allow the chondrocytes to aggregate into a cartilaginous biomass that can withstand the shear stresses of constant perfusion. To prevent the issue of contamination the cells should be statically cultured inside the bioreactor chamber for four weeks prior to perfusion. Also both directions of vertical perfusion should be explored in the future; upwards to reconfirm the results of Method 3 and downward to explore the effects of the added compressive force of the cells against the transwell insert membrane.

4. Conclusions

In summary, our novel through-thickness perfusion bioreactor has shown the capacity to successfully generate a 24 mm diameter scaffold-free tissue engineered cartilage construct with superior biochemical and biomechanical properties to a statically cultured cartilage construct. The downside is that, currently, the bioreactor is unreliable in its ability to repeatedly produce scaffold-free tissue engineered constructs of high biochemical and biomechanical properties. It is apparent that the design of the bioreactor is sound, yet the procedure of using the bioreactor needs refinement and further exploration.

In future experiments, the neonatal porcine chondrocytes should be cultured *ex vivo* immediately inside the bioreactor under static conditions for at least a 28 day period. With the bioreactor designed to maintain sterility, this provides a more desirable culture environment than previously used for static culture in experiments. Variability of the perfusion duration after static conditioning should also be explored using both directions of flow. By using either a different peristaltic pump with a lower minimum speed, or by using larger gage tubing, could also help reduce flow speed and will likely reduce cell culture duration in the future.

Author Contributions

Eric Gilbert contributed with conduction of all experiments, acquisition of data, analysis and interpretation of data, and drafting the article. Mark Mosher contributed with the acquisition of biomechanical data. Anuhya Gottipati contributed with the acquisition of histological data. Steven Elder contributed with conception and design, analysis and interpretation of data, and drafting the article.

Conflicts of Interest

The authors declare no conflict of interest.

References

1. Nukavarapu, S.; Dorcenus, D. Osteochondral tissue engineering: Current strategies and challenges. *Biotechnol. Adv.* **2013**, *31*, 706–721.
2. Kahn, I.M.; Singhrao, S.K.; Duance, V.S.; Archer, C.W. Cartilage integration: Evaluation of the reasons for failure of integration during cartilage repair. A Review. *Eur. Cells Mater.* **2008**, *16*, 26–39.
3. Perera, J.R.; Gikas, P.D.; Bentley, G. The present state of treatments for articular cartilage defects in the knee. *Ann. R. Coll. Surg. Engl.* **2012**, *94*, 381–387.
4. Bhosale, A.M.; Richardson, J.B. Articular cartilage: Structure, injuries and review of management. *Br. Med. Bull.* **2008**, *87*, 77–95.
5. Darling, E.; Athanasiou, K. Articular cartilage bioreactor and bioprocesses. *Tissue Eng.* **2003**, *9*, 9–26.
6. Chen, H.-C.; Hu, Y.-C. Bioreactors for tissue engineering. *Biotechnol. Lett.* **2006**, *28*, 1415–1423.
7. Athanasiou, K.A.; Darling, E.M.; Hu, J.C. *Articular Cartilage Tissue Engineering: Synthesis Lectures on Tissue Engineering*; Morgan & Claypool: Fort Collins, CO, USA, 2010; Volume 3.

8. Elder, S.H.; Cooley, A.J., Jr.; Borazjani, A.; Sowell, B.L.; To, H.; Tran, S.C. Production of hyaline-like cartilage by bone marrow mesenchymal stem cells in a self-assembly model. *Tissue Eng. Part A* **2009**, *15*, 3025–3035.
9. Naumann, A.; Dennis, J.E.; Aigner, J.; Coticchia, J.; Arnold, J.; Berghaus, A.; Kastenbauer, E.R.; Caplan, A.I. Tissue engineering of autologous cartilage grafts in three-dimensional *in vitro* macroaggregate culture system. *Tissue Eng.* **2004**, *10*, 1695–1706.
10. Hu, J.C.; Athanasiou, K.A. A self-assembling process in articular cartilage tissue engineering. *Tissue Eng.* **2006**, *12*, 969–979.
11. Murdoch, A.D.; Grady, L.M.; Ablett, M.P.; Katopodi, T.; Meadows, R.S.; Hardingham, T.E. Chondrogenic differentiation of human bone marrow stem cells in transwell cultures: Generation of scaffold-free cartilage. *Stem Cells* **2007**, *25*, 2786–2796.
12. Campbell, A.B.; Knopp, M.V.; Kolovich, G.P.; Wei, W.; Jia, G.; Siston, R.A.; FLanigan, D.C. Preoperative MRI underestimates articular cartilage defect size compared with an arthroscopic knee surgery. *Am. J. Sports Med.* **2013**, *41*, 590–595.
13. Salzmann, G.M.; Sah, B.; Südkamp, N.P.; Niemeyer, P. Clinical outcome following the first-line, single lesion microfracture at the knee joint. *Arch. Orthop. Trauma Surg.* **2013**, *133*, 303–310.
14. Santoro, R.; Olivares, A.L.; Brans, G.; Wirz, D.; Longinotti, C.; Lacroix, D.; Martin, I.; Wendt, D. Bioreactor based engineering of large-scale human cartilage grafts for joint resurfacing. *Biomaterials* **2010**, *31*, 8946–8952.
15. Furukawa, K.S.; Sato, M.; Nagai, T.; Ting, S.; Mochida, J.; Ushida, T. *Scaffold-free Cartilage Tissue by Mechanical Stress Loading for Tissue Engineering*; Eberli, D., Ed.; InTech: Winchester, UK, 2010. Available online: <http://www.intechopen.com/books/tissue-engineering/scaffold-free-cartilage-tissue-by-mechanical-stress-loading-for-tissue-engineering> (accessed on 13 March 2013).
16. Mohanraj, B.; Farran, A.J.; Mauck, R.L.; Dodge, G.R. Time-dependent functional maturation of scaffold-free cartilage tissue analogs. *J. Biomech.* **2014**, *47*, 2137–2142.
17. Vunjak-Novakovic, G.; Obradovic, B.; Treppo, S.; Grodzinsky, A.J.; Langer, R.; Freed, L.E. Bioreactor cultivation conditions modulate the composition and mechanical properties of tissue-engineered cartilage. *J. Orthop. Res.* **1999**, *17*, 130–138.
18. Mizuno, S.; Allemann, F.; Glowacki, J. Effect of medium perfusion on matrix production by bovine chondrocytes in three-dimensional collagen sponges. *J. Biomed. Mater. Res.* **2001**, *56*, 368–375.
19. Raimondi, M.T.; Easton, S.M.; Laganà, M.; Aprile, V.; Nava, M.M.; Cerullo, G.; Osellame, R. Three-dimensional structural niches engineered via two-photon laser polymerization promote stem cell homing. *Acta Biomater.* **2013**, *9*, 4579–4584.
20. Laganà, M.; Raimondi, M.T. A miniaturized, optically accessible bioreactor for systematic 3D tissue engineering research. *Biomed. Microdevices* **2012**, *14*, 225–234.
21. Schulz, R.M.; Bader, A. Cartilage tissue engineering and bioreactor systems for the cultivation and stimulation of chondrocytes. *Eur. Biophys. J.* **2007**, *36*, 539–568.
22. Julkunen, P.; Korhonen, R.K.; Herzog, W.; Jurvelin, J.S. Uncertainties in indentation testing of articular cartilage: A fibril-reinforced poroviscoelastic study. *Med. Eng. Phys.* **2008**, *30*, 506–515.
23. Haynes, W.C.; Keer, L.M.; Herrmann, G.; Mockros, L.F. A mathematical analysis for indentation tests of articular cartilage. *J. Biomech.* **1972**, *5*, 541–551.

24. Reddy, G.K.; Enwemeka, C.S. A simplified method for the analysis of hydroxyproline in biological tissues. *Clin. Biochem.* **1996**, *29*, 225–229.
25. Hoemann, C. Molecular and biochemical assays of cartilage components. In *Methods in Molecular Medicine: Cartilage and Osteoarthritis*; Ceuninck, F., Sabatini, M., Pastoureau, P., Eds.; Humana Press: Totowa, NJ, USA, 2004; Volume 2, pp. 127–156.
26. Loba, E.G.; Wren, T.A.; Beaupré, G.S.; Carter, D.R. Mechanobiology of soft skeletal tissue differentiation—A computational approach of a fiber-reinforced poroelastic model based on homogeneous and isotropic simplifications. *Biomech. Model. Mechanobiol.* **2003**, *2*, 83–96.
27. Ryu, J.; Saito, S.; Yamamoto, K. Changes in articular cartilage in experimentally induced patellar subluxation. *Ann. Rheum. Dis.* **1997**, *56*, 677–681.
28. Raimondi, M.T. Engineered tissue as a model to study cell and tissue function from a biophysical perspective. *Curr. Drug Discov. Technol.* **2006**, *3*, 245–268.
29. Sacco, R.; Causin, P.; Zunino, P.; Raimondi, M.T. A multiphysics/multiscale 2D numerical simulation of scaffold-based cartilage regeneration under interstitial perfusion in a bioreactor. *Biomech. Model. Mechanobiol.* **2010**, *10*, 577–589.
30. Grad, S.; Eglin, D.; Alini, M.; Stoddart, M. Physical stimulation of chondrogenic cells *in vitro*: A review. *Clin. Orthop. Relat. Res.* **2011**, *469*, 2764–2772.
31. Mabvuure, N.; Hindocha, S.; Khan, W. The role of bioreactors in cartilage tissue engineering. *Curr. Stem Cell Res. Ther.* **2013**, *7*, 287–292.
32. Sun, S.; Ren, Q.; Wang, D.; Zhang, L.; Wu, S.; Sun, X. Repairing cartilage defects using chondrocyte and osteoblast composites developed using a bioreactor. *Chin. Med. J.* **2011**, *124*, 758–763.
33. Gharravi, A.M.; Orazizadeh, M.; Ansari-Asl, K.; Banoni, S.; Izadi, S.; Hashemitabar, M. Design and fabrication of anatomical bioreactor systems containing alginate scaffolds for cartilage tissue engineering. *Avicenna J. Med. Biotechnol.* **2012**, *4*, 65–74.
34. Pazzano, D.; Mercier, K.; Moran, J.; Fong, S.; DiBiasio, D.; Rulfs, J.; Kohles, S.; Bonassar, L. Comparison of chondrogenesis in static and perfused bioreactor culture. *Biotechnol. Prog.* **2000**, *16*, 893–896.